DOI: 10.1002/ejic.201100168

Switchable Green and White Luminescence in Terbium-Based Ionic Liquid Crystals

Anna Getsis[a] and Anja-Verena Mudring*[a]

Dedicated to John D. Corbett on the occasion of his 85th birthday

Keywords: Ionic liquids / Ionic liquid crystals / Liquid crystals / Lanthanides / Luminescence

[C_{12}mim]Br (C_{12}mim = 1-dodecyl-3-methyl) and [C_{12}mpyr]Br (C_{12}mpyr = *N*-dodecyl-*N*-methylpyrrolidinium), both doped with $TbBr_3$, as well as the neat compounds $[C_{12}mim]_3[TbBr_6]$ and $[C_{12}mpyr]_3[TbBr_6]$ show mesomorphic behavior and are able to form smectic liquid crystalline phases. The thermal phase behavior of all compounds was investigated by hot-stage polarizing optical microscopy and differential scanning calorimetry. Whilst the doped compounds crystallize around room temperature, the neat compounds solidify as glasses around –5 °C and qualify also as ionic liquids. The crystal structure of the acetonitrile solvate of the imidazolium compound, $[C_{12}mim]_3[TbBr_6]\cdot 2CH_3CN$, could be determined by single X-ray diffraction. The structure features alternating double layers of $[C_{12}mim]^+$ cations and $[TbBr_6]^{3-}$ octahedra with hydrogen bonded acetonitrile. $[C_{12}mim]_3[TbBr_6]\cdot 2CH_3CN$ can serve as a structure model for the smectic mesophase of the solvate-free $[C_{12}mim]_3[TbBr_6]$. All materials show strong green luminescence from the $^5D_4$-level of Tb^{3+} after excitation into the $4f^8 \rightarrow 4f^75d^1$ transition. In case of the imidazolium compounds, the color of this emission can be switched between green and blue-white depending on the excitation energy. After excitation with λ_{ex} = 254 nm, strong green emission mainly from the $^5D_4$-level of Tb^{3+} is observed. With λ_{ex} = 366 nm, only the blue-white luminescence from the imidazolium cation itself is detected.

Introduction

Ionic liquids (ILs) have attracted substantial interest in recent years.[1] They may feature properties such as negligible vapor pressure, wide liquid range, good thermal stability, considerable electric conductivity, and a wide electrochemical window. These properties and especially the unique property combinations have shown to be advantageous for a large number of applications. Today, ILs are predominantly used in separation, various electrochemical applications, organic synthesis, and catalysis.[2] As salts, ionic liquids are composed of distinct cations and anions, which make them widely tunable. The variety of cation/anion combinations has led to the denomination of ILs as "designer solvents".[1] Indeed, they may be designed for specific applications by choosing the appropriate cation and anion combination.

Ionic liquids that contain one or two anisotropically shaped ions (rodlike or disklike) are likely to form mesophases. Such compounds that are able to form liquid crystals can be addressed as ionic liquid crystals (ILCs). They combine the properties of typical ionic liquids with those of liquid crystals. However, ILCs feature some properties, such as ionic conductivity, which are not encountered in classical LCs consisting of neutral molecules. Recently, it was shown that double alkyl-substituted imidazolium ILCs show strong non-Newtonian fluidic behavior in the LC state, while they are Newtonian liquids in the liquid (IL) state.[3] Derivatized *N*-methylimidazolium cations are by far the most popular cations used for both ILs and ILCs.[3,4,5] It is known that certain 1-alkyl-3-methylimidazolium salts with long alkyl side chains can form lamellar mesophases. The mesophase stability increases with increasing length of the alkyl chain.[3,4] However, aside from changing the substituents on the imidazolium rings or coupling imidazolium rings with use of different spacers, the charged head group can be varied. Recently, pyrrolidinium ionic liquids attracted attention because of their good thermal and electrochemical stability.[6]

Metal-containing liquid crystals (metallomesogens) form a special class of ILCs. By choosing a suitable metal ion as constituent of the ILC, additional functionalities that originate from the metals, such as redox activity, magnetism, or luminescence, can be introduced to the material. In consequence, multifunctional materials are obtained. Several reviews survey the intensive studies on neutral, uncharged

[a] Anorganische Chemie I, Ruhr-Universität Bochum, Universitätsstrasse 150, 44801 Bochum, Germany
Fax: +49-234-27408
E-mail: anja.mudring@rub.de
http://www.anjamudring.de

Supporting information for this article is available on the WWW under http://dx.doi.org/10.1002/ejic.201100168.

 © 2011 Wiley-VCH Verlag GmbH & Co. KGaA, Weinheim

metallomesogens.[7] In contrast, studies of ionic metallomesogens have been neglected until recently.[8,9] However, metal-containing ionic liquids (ILs) have received substantial attention and combining the materials properties of metal-containing ILs[10] and liquid crystals appears to open up perspectives for new materials. A special interest in the field of metal-containing liquid crystals focuses on light-emitting liquid crystals for potential applications in emissive LC displays.[11] By incorporating cations of the 4f elements, such as Tm^{3+} (blue), Eu^{3+} (red), and Tb^{3+} (green), LCs emitting in the three basic colors can be obtained.[10,12] In addition, aligned luminescent LCs can emit polarized light.[13] A high magnetic anisotropy of the lanthanide ion, as found for Tb^{3+}, Dy^{3+}, and Tm^{3+}, makes the alignment of the mesophase in an external magnetic field possible.[14] Thus, such compounds might be of interest for applications in electrically and magnetically switchable devices.

Here we report on the synthesis as well as on the structural, thermal, and photophysical behavior of 1-dodecyl-3-methylimidazolium bromide and *N*-methyldodecylpyrrolidinium bromide doped with terbium(III) bromide, $6[C_{12}mim]Br{\cdot}[C_{12}mim]_3[TbBr_6]$ (**1a**) (C_{12}mim = 1-dodecyl-3-methyl) and $6[C_{12}mpyr]Br{\cdot}[C_{12}mpyr]_3[TbBr_6]$ (**2a**) (C_{12}mpyr = *N*-dodecyl-*N*-methylpyrrolidinium), as well as the neat terbium ionic liquid crystals $[C_{12}mim]_3[TbBr_6]$ (**1b**) and $[C_{12}mpyr]_3[TbBr_6]$ (**2b**), and the structure of the related acetonitrile solvate $[C_{12}mim]_3[TbBr_6]{\cdot}2CH_3CN$ (**1c**) (Table 1).

Table 1. Compounds studied.

Compound number	Formula
1a	$6[C_{12}mim]Br \cdot [C_{12}mim]_3[TbBr_6]$
1b	$[C_{12}mim]_3[TbBr_6]$
1c	$[C_{12}mim]_3[TbBr_6]{\cdot}2CH_3CN$
2a	$6[C_{12}mpyr]Br{\cdot}[C_{12}mpyr]_3[TbBr_6]$
2b	$[C_{12}mpyr]_3[TbBr_6]$

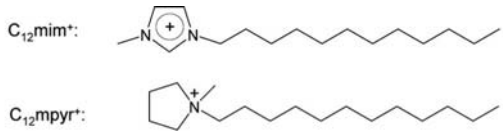

Results and Discussion

Crystal Structure of $[C_{12}mim]_3[TbBr_6]{\cdot}2CH_3CN$

Several attempts employing various techniques to grow crystals of neat hexabromoterbate complexes {$[C_{12}mim]_3[TbBr_6]$ (**1b**) and $[C_{12}mpyr]_3[TbBr_6]$ (**2b**)} with sufficient quality for X-ray structure analysis failed. However, needle-shaped, colorless single crystals of the acetonitrile monosolvate of **1b**, $[C_{12}mim]_3[TbBr_6]{\cdot}2CH_3CN$ (**1c**), could be grown from an acetonitrile solution of **1b** at 5 °C. Single-crystal X-ray diffraction structure analysis reveals that the compound crystallizes in the orthorhombic space group *Pbca* (no. 61) [a = 14.979(4) Å, b = 18.500(5) Å, c = 50.11(2) Å, Z = 8, V = 13885(7) Å^3] (Table S1 in the Supporting Information). $[C_{12}mim]_3[TbBr_6]{\cdot}2CH_3CN$ is isotypic with the dysprosium analogue, $[C_{12}mim]_3[DyBr_6]{\cdot}2CH_3CN$.[15] As expected from the lanthanide contraction, the molar volume of $[C_{12}mim]_3[TbBr_6]{\cdot}2CH_3CN$ (**1c**) is larger than that of the dysprosium compound (1736 Å^3 vs. 1677 Å^3). The asymmetric unit of **1c** contains three crystallographically independent $[C_{12}mim]^+$ cations, one $[TbBr_6]^{3-}$ unit, and two acetonitrile molecules. Tb^{3+} is coordinated in an almost ideally octahedral manner by six bromide ions. The Tb–Br interatomic distances range from 2.801 to 2.868 Å (see Supporting Information), which are slightly longer than typical inorganic salts with complex $[TbBr_6]^{3-}$ anions. For example, in $Cs_3[Tb_2Br_9]$, values of 2.697–2.902 Å are found.[16] A similar observation was made in case of the $[C_{12}mim]_3[DyBr_6]{\cdot}2CH_3CN$. Bonding distances and angles for the 1-dodecyl-3-methylimidazolium cations in **1c** are in the expected range and can be compared to those in $[C_{12}mim]_3[DyBr_6]{\cdot}2CH_3CN$ or to similar short-chain *N*-*n*-alkyl-*N*-methylimidazolium compounds.[17] Two of the dodecyl chains adopt *all-trans* conformation, while the third reveals a *gauche* conformation around the C7–C8 bond. Such crank-handle-like arrangements have also been observed in related hexafluorophosphate salts, $[C_n mim][PF_6]$ (n = 12, 14, 16).[18] In **1c**, the cations themselves form rows that are stacked along the *a* axis in such a way that their alkyl tails alternate in orientation in neighboring layers, and thereby a double layer is formed (Figure 1). Within the layers, structural segregation into hydrophilic and hydrophobic domains occurs. The hydrophobic parts are built up by interdigitated *n*-alkyl tails of the imidazolium cation. The charged imidazolium head groups, together with the hexabromoterbate octahedra, form the hydrophilic part of the structure. Within a layer, each $[TbBr_6]^{3-}$ anion is surrounded by six $[C_{12}mim]^+$ cations and two acetonitrile molecules. Nonclassical hydrogen bonds formed by (NN)-

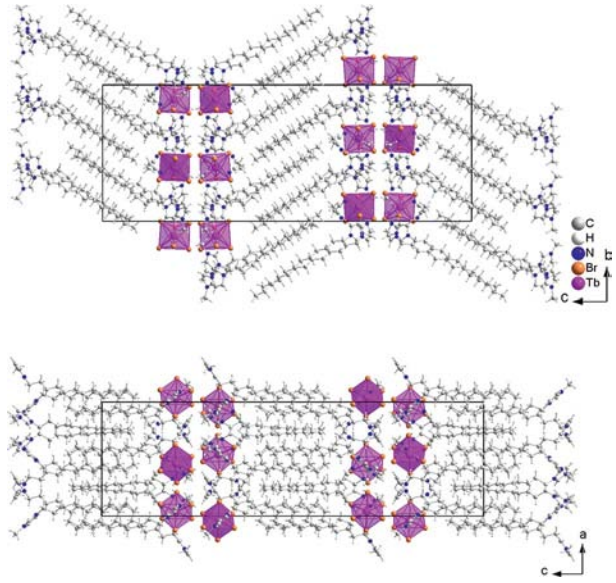

Figure 1. Crystal structure of $[C_{12}mim]_3[TbBr_6]{\cdot}2CH_3CN$ (**1c**): view along the crystallographic *a* axis (top) and along the crystallographic *b* axis (bottom).

 © 2011 Wiley-VCH Verlag GmbH & Co. KGaA, Weinheim

$Csp^2\cdots Br$ and $(NC)Csp^2\cdots Br$ interactions (see Supporting Information), which are shorter than the commonly accepted limiting values of 3.72 Å and 3.75 Å,[19] exist not only within the hydrophilic parts of each layer but also between them. The structural features of **1c** already suggest the possibility of the formation of a smectic mesophase. Unfortunately, the compound looses acetonitrile before such a phase transition would occur. However, the structure of **1c** together with the structures of $[C_{12}mim]Br\cdot H_2O$[20] and $[C_{12}mpyr]Br$[6b] are valuable structural models for the mesophases adopted by 1-dodecyl-3-methylimidazolium bromide and *N*-methyl-dodecylpyrrolidinium bromide doped with terbium bromide (**1a** and **2a**) as well as for 1-dodecyl-3-methylimidazolium hexabromoterbate(III) (**1b**) *N*-methyl-*N*-dodecylpyrrolidinium hexabromoterbate(III) (**2b**).

Vibrational Spectroscopy

Far-infrared (FIR) and Raman spectra recorded for all samples show the expected vibrations for the respective cation and anion (Figure 2 and Supporting Information). The characteristic vibrations of the $[TbBr_6]^{3-}$ octahedron prove that reaction of $TbBr_3$ with the respective bromide ILCs leads to the formation of the complex hexabromoterbate anion and justifies the formulation of the compounds as $6[C_{12}mim]Br\cdot[C_{12}mim]_3[TbBr_6]$ (**1a**) and $6[C_{12}mpyr]Br\cdot[C_{12}mpyr]_3[TbBr_6]$ (**2a**). The unsymmetrical stretching vibration (F_{1u}) can be detected in the far infrared spectrum at 159 cm^{-1} for **1a** and **1b** and 167 cm^{-1} for **2a** and **2b**. The symmetrical stretching vibration (A_{1g}) can be observed in the Raman spectrum. For **1b** and **2b**, the A_{1g} vibration is found at 154 and 157 cm^{-1}, respectively. The Raman spectrum of **2a** looks like a superposition of the Raman spectra of $[C_{12}mpyr]_3[TbBr_6]$ and $[C_{12}mpyr]Br$, which is another piece of evidence that $6[C_{12}mpyr]Br\cdot[C_{12}mpyr]_3[TbBr_6]$ (**2a**) is a good formula representation for the $C_{12}mpyr$ system doped with $TbBr_3$.

Through Raman spectroscopy it is also possible to distinguish crystalline, mesomorphous, and amorphous ordering.[21] As the phase behavior of alkyl chains in polymers has been well studied, this knowledge can be used to interpret the spectra of **1** and **2**. Comparing the Raman spectrum of $[C_{12}mim]_3[TbBr_6]$ in the region 1400–1500 cm^{-1} (Figure 3) with the typical spectrum of a partially crystalline polymer (polyethylene, PE; Figure 3, inset) reveals great similarities and confirms the low degree of ordering in the alkyl chains in the liquid crystalline state. For a crystalline material, distinctly split lines of significantly lower line width would be expected. In addition, the conformation of the alkyl side chains can be elucidated. Combined experi-

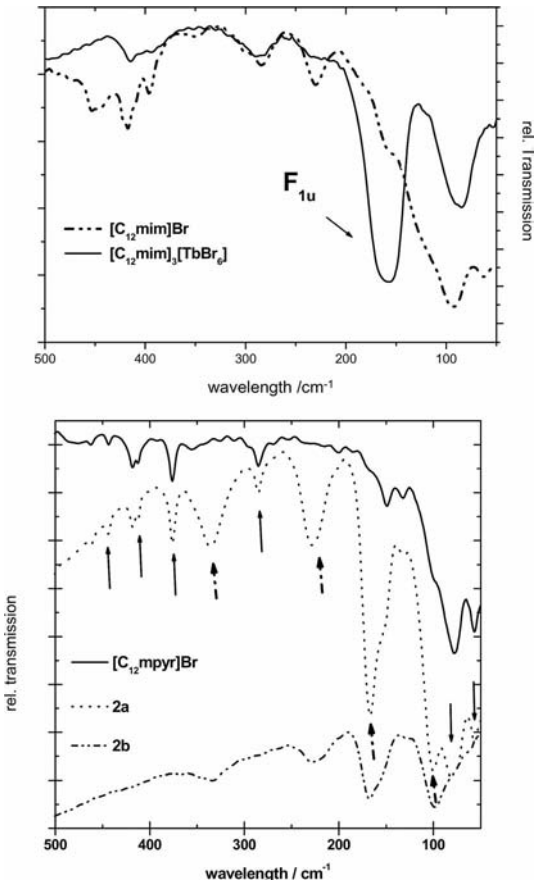

Figure 2. FIR spectra of the Tb-containing ILCs **1b** (top), **2b**, and **2a** (bottom) in comparison with those of neat $[C_{12}mim]Br$ and $[C_{12}mpyr]Br$.

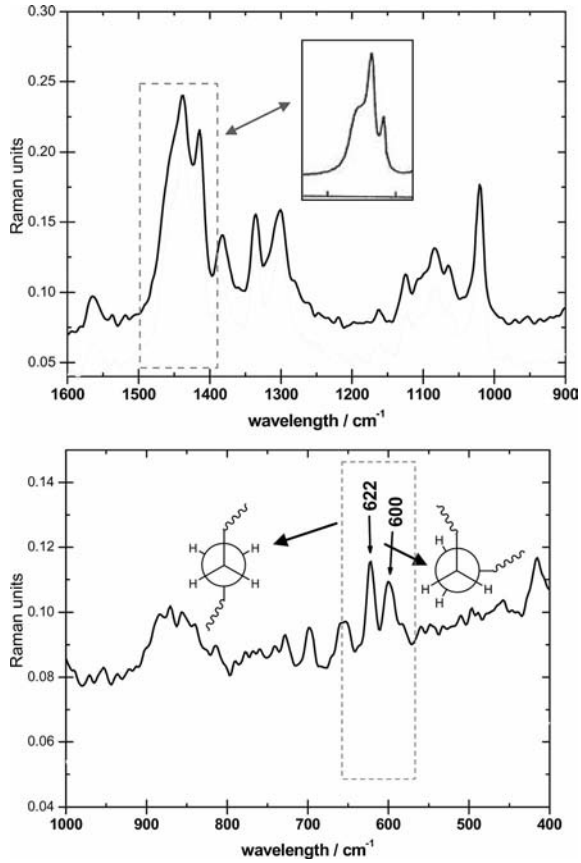

Figure 3. Details of the Raman spectrum of **1b**.

 © 2011 Wiley-VCH Verlag GmbH & Co. KGaA, Weinheim

mental and theoretical Raman investigations of various 1-butyl-3-methylimidazolium salts show that *all-trans* conformers should give a broad signal at about 625 cm^{-1} while the *gauche* conformer should show a band at about 603 cm^{-1}. Both features can be detected in the Raman spectrum of $[C_{12}mim]_3[TbBr_6]$ (Figure 3, bottom.).

Thermal Analysis

The thermal properties of **1a**, **1b**, **2a**, and **2b** were examined by polarizing optical microscopy (POM) and differential scanning calorimetry (DSC). The DSC traces of the cooling and heating cycles and the respective POM pictures are shown in Figures 4 and 5. Exact transition temperatures and corresponding enthalpy changes are given in the Supporting Information. The highest thermal invent always corresponds to the clearing point. In case of the imidazolium compounds, the clearing point is only marginally higher than that of neat C_{12}mimBr (Figure 4). Whilst **1b** maintains its liquid crystalline state to low temperatures and only undergoes a glass transition at about –6 °C upon cooling, for **1a** a liquid-crystal-to-solid (LC–S) transition is found at roughly the same temperature as that of $[C_{12}mim]$-Br. Likewise the DSC traces of **2a** and $[C_{12}mypr]$Br bear close resemblances (Figure 5). The three thermal changes occurring between 120 °C and 55 °C are due to LC–LC phase transitions. At 54.2 °C crystallization occurs. The thermal behavior of **1b** is similar to that of **2b**. After conversion from the isotropic liquid to the liquid crystalline state upon cooling, no crystallization but rather a glass transition takes place at –5 °C. The clearing points of the imidazolium compounds, **1a** and **1b**, are several tens of degrees lower than those of the pyrrolidinium analogues. Also, the glass transition and crystallization temperatures are found at lower values for the imidazolium compounds. In summary, all compounds show an appreciable LC window including the room temperature range. The phase transitions of the imidazolium compounds take place at lower temperatures than those of the pyrrolidinium analogues.

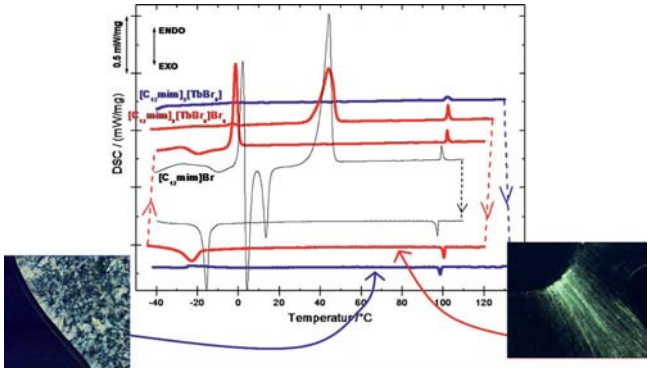

Figure 4. DSC thermogram of **1a** (in red) and **1b** (in blue) with corresponding POM micrographs in comparison to the thermogram of neat $[C_{12}mim]$Br.

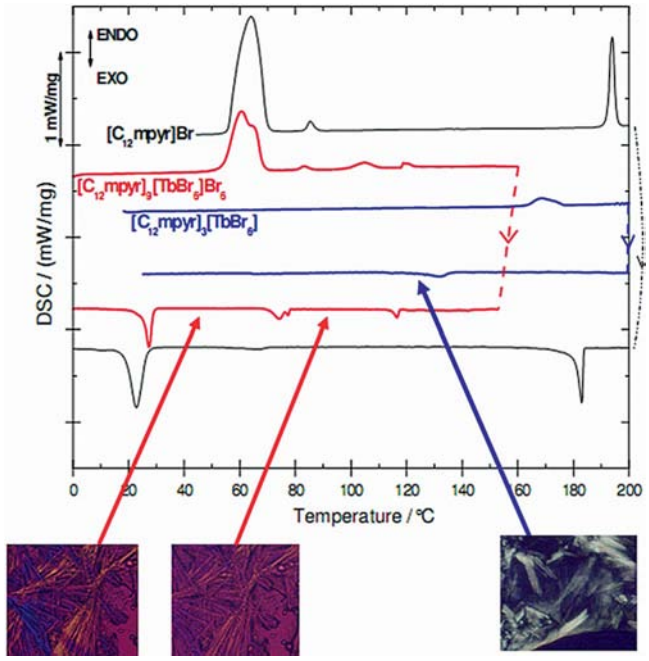

Figure 5. DSC-thermogram of **2a** (in red) and **2b** (in blue) with corresponding POM micrographs in comparison to the thermogram of neat $[C_{12}mpyr]$Br.

It not easy to observe unambiguous defect textures for mesophases of imidazolium- and pyrrolidinium-based ILCs by polarizing optical microscopy, as these compounds show a strong tendency to form spontaneously single homeotropic monodomains, which results in dark fields between the crossed polarizers of the microscope. It is extremely difficult to disturb this alignment in order to get more meaningful textures.[22,23] The dilemma is further enhanced by the fact that all compounds are extremely air-sensitive and have to be handled under strictly inert conditions. However, POM investigations confirm that the highest thermal events measured by DSC correspond to the clearing point. The optical textures observed on cooling from the isotropic melt, as fan-shaped, oily-streaky forms and bâtonnetes, are characteristic for smectic mesophases. Judging from the bilayered crystal structure of $[C_{12}mim]Br{\cdot}H_2O$,[20] $[C_{12}mpyr]$-Br,[6b] and $[C_{12}mim]_3[DyBr_6]{\cdot}2CH_3CN$,[15] it seems quite likely that all compounds form smectic mesophases. Indeed, smectic phases are typical of 1-*n*-alkylimidazolium ILCs.[4,24] This behavior is possibly due to the fact that the layer structure originates not only from the hydrophobic van der Waals interactions between the long cation–alkyl tails but is strongly stabilized by Coulomb interactions in the hydrophilic part of the structure where the charged cation head groups and the anions are located. In consequence, the alkyl tails can melt independently from the layers and several smectic phases can be adopted due to the different space requirements of the alkyl tails with rising freedom as well as their orientation towards the layer normal. Unfortunately, we were experimentally not able to carry out temperature-dependent SAXS measurements under strictly anhydrous conditions so far.

 © 2011 Wiley-VCH Verlag GmbH & Co. KGaA, Weinheim

Luminescence Spectroscopy

Tb^{3+} is known to be an efficient emitter of green light originating from electronic transitions from the $^5D_4$ level to the ^7F_J multiplet of the ground state.[25] Important for efficient luminescence is the effective excitation of Tb^{3+}. However, trivalent lanthanide cations generally have a low absorption coefficient. Yet, Tb^{3+} can be efficiently excited with far-UV light, as it features $4f^n \rightarrow 4f^{n-1}5d^1$ transitions at low energies with appreciable absorption. In compounds containing $[TbBr_6]^{3-}$, the $4f^n \rightarrow 4f^{n-1}5d^1$ transition is known to take place around 36000 cm^{-1} (ca. 278 nm).[26]

The excitation as well as the emission spectra of **1a**, **2a**, **1b**, and **2b** show the characteristic transitions for Tb^{3+} (Figure 6).[27] The emission spectra of the imidazolium and the pyrrolidinium ILCs show the same transitions in the same energy range with the same relative intensities. This applies not only to the f–f transitions but also to the f–d transition, which is found at about 282–289 nm. This points to the same local coordination environment for Tb^{3+} in all compounds and confirms the presence of $[TbBr_6]^{3-}$.

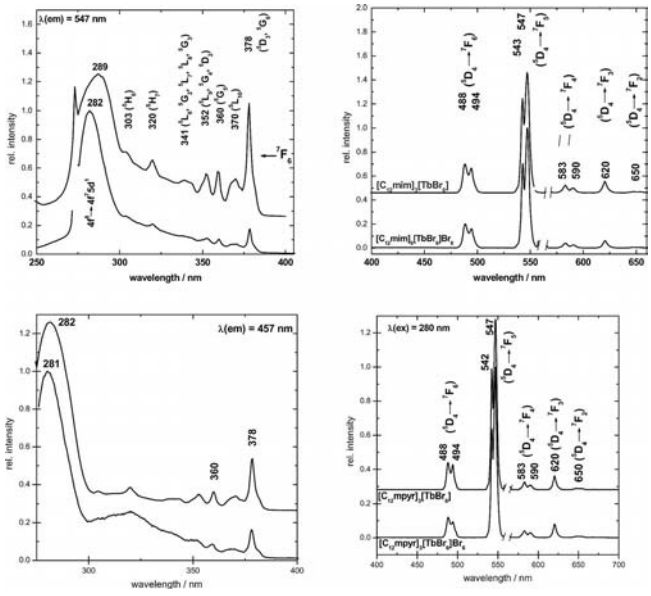

Figure 6. Normalized excitation spectra (monitored at λ_{em} = 547 nm, left) and emission spectra under excitation of the $4f^7d^1$ transition (right) for **1a** and **1b** (top) as well as for **2a** and **2b** (bottom).

All compounds show an efficient green light emission with long lifetimes of the excited $^5D_4$ level. The lifetimes of the pyrrolidinium compounds are somewhat higher (4.4 ms for **2a** and 4.0 ms for **2b**) compared to those of the corresponding imidazolium ILCs (3.3 ms for **1a** and 3.7 ms for **2b**). However, in case of the imidazolium compounds, the light emission is more intense than that of the pyrrolidinium compounds. This is due to an energy transfer from the imidazolium cation to the Tb^{3+} ion. Such an influence has been reported previously.[9b] Furthermore, in case of the imidazolium salts, it is possible to tune the emission color between white and green depending on the excitation wavelength (Figure 7).

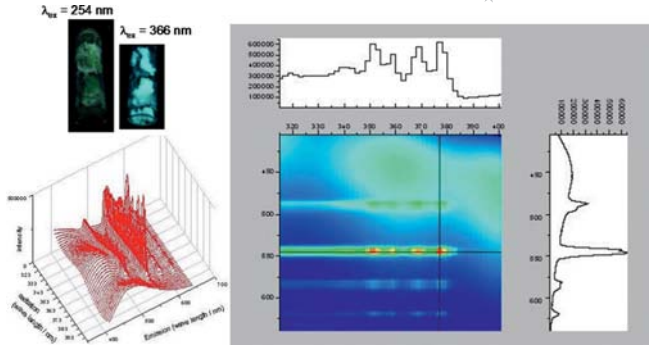

Figure 7. 2D emission–excitation spectra of **1a**.

Excitation with UV light of short wavelength leads to an efficient activation of the Tb^{3+} ion, and the sample appears green due to the high intensity of the $^5D_4 \rightarrow {}^7F_6$ emission around 545 nm. Excitation with longer wavelengths (> 390 nm) leads to strong, broad emission in the blue region of light originating from the imidazolium cation. The Tb^{3+} cation can no longer be sensitized. Similar behavior has recently been reported for the ionic liquid crystal compound $[C_{12}mim]Cl$ when doped with Eu^{3+} (red to bluish-white) as well as for $[C_{12}mim]_3[DyBr_6]$ (yellow-orange to blue-white).[28]

Conclusions

$[C_{12}mim]_3Br$ and $[C_{12}mpyr]Br$, both doped with $TbBr_3$ (**1a** and **2a**), as well as the neat compounds $[C_{12}mim]_3[TbBr_6]$ (**1b**) and $[C_{12}mpyr]_3[TbBr_6]$ (**2b**), are interesting new materials as they are able to form mesophases over a wide temperature range. Whilst **1a** and **2a** crystallize around room temperature and have clearing points around 100 °C and 190 °C, respectively, the neat compounds **1b** and **2b** solidify as liquid crystal glasses around –5 °C. The neat compounds $[Cat]_3[TbBr]_6$ (Cat = $C_{12}mim$, $C_{12}mpyr$) essentially show the same clearing points as the doped materials **1a** and **2a**. The thermal phase behavior of all compounds was investigated not only by differential scanning calorimetry but also by hot-stage polarizing optical microscopy in order to get more insight into the nature of the formed mesophases. For all phases, textures indicating to smectic mesophases were found. Unfortunately, we did not succeed in obtaining reliable temperature-dependent SAXS data, as all compounds are highly moisture-sensitive. However, we were able to determine the crystal structure of the acetonitrile solvate $[C_{12}mim]_3[TbBr_6]\cdot 2CH_3CN$ (**1c**), which might serve as a structural model. Compound **1c** forms a layered structure in which double layers of hydrophilic and hydrophobic structure regions alternate. The hydrophobic structure parts are formed by interdigitated dodecyl tails of imidazolium cations with different orientation. The hydrophilic structure regions are built up by the charged imidazolium head groups and octahedral hexabromodysprosiate(III) complex anions together with hydrogen-bonded acetonitrile. It is anticipated that the ion arrangement is largely retained when the solvate acetonitrile molecules are lost.

 © 2011 Wiley-VCH Verlag GmbH & Co. KGaA, Weinheim

All materials show a strong green luminescence from the $^5D_4$ level upon excitation of the $4f^8 \rightarrow 4f^7 5d^1$ transition of Tb^{3+}. In case of the imidazolium compounds, the color of this emission can be switched between green and blue-white depending on the excitation energy used. After excitation with λ_{ex} = 254 nm, strong green emission mainly from the $^5D_4$ level of Tb^{3+} is observed. With λ_{ex} = 366 nm excitation, only the bluish-white luminescence from the imidazolium cation itself is detected.

Experimental Section

General Remarks: Synthesis and sample handling were carried out under strictly inert conditions by using standard Schlenk and argon glove box techniques. All solvents were dried by using standard procedures. [C_{12}mim]Br and [C_{12}mpyr]Br were prepared according to literature procedures.[6b,20]

Terbium Tribromide ($TbBr_3$): $TbBr_3$ was synthesized according to a modified literature procedure.[29] Terbium(III,IV) oxide (2.00 g, 0.0027 mol, 99.9% Fluka Chemie AG, Buchs, CH) and ammonium bromide (6.40 g, 0.0648 mol, suprapur® 99.995% Merck, Darmstadt, D) were dissolved in aqueous hydrobromic acid (48%, Aldrich, Steinheim, D). The formed $(NH_4)_3TbBr_6 \cdot xH_2O$ was decomposed to $TbBr_3$ at 900 °C. At this temperature any excess ammonium bromide sublimes off. Crude $TbBr_3$ is then purified by sublimation under vacuum ($< 10^{-5}$ mbar) at 920 °C. The purity of $TbBr_3$ was checked by powder XRD (Mo-K_α, Huber Image Plate, Rimsting, D).

1a, 1b, 2a, and 2b: These compounds were obtained by reacting the respective amounts of $TbBr_3$ with [C_{12}mim]Br or [C_{12}mpyr]Br at 120 °C. After cooling to room temperature, highly viscous bulk products were obtained. Single crystalline **1c** formed after cooling a solution of **1b** in dry acetonitrile to 5 °C. The thermolabile compound loses the solvate acetonitrile below room temperature.

^{1}H NMR Spectroscopy: Nuclear magnetic resonance (NMR) spectra were recorded with a Bruker AC-300 spectrometer (operating at 300 MHz for ^{1}H, Bruker Germany GmbH, D).

IR-Raman Spectroscopy: IR spectra of the solid were recorded with a IFS-66V-S Fourier Transform IR spectrometer (Bruker Optik GmbH, Ettlingen, D); samples to be measured were pressed in a polyethylene matrix for the far IR range (50–600 cm^{-1}) and in a KBr matrix for the middle IR (MIR) range (600–4000 cm^{-1}). Raman spectra were recorded with a FRA 106-S Fourier Transform Raman spectrometer (Bruker Optik GmbH, Ettlingen, D) at 150 mW. Raman samples were measured in glass capillaries with an inner diameter of 0.1 cm and a wall thickness of 0.15 mm.

Luminescence Spectroscopy: Excitation and emission spectra and also luminescence decays were recorded with a Jobin Yvon Horiba Fluorolog FL3–22 with a xenon lamp as the excitation source and a photomultiplier for detection.

Thermal Measurements: Differential scanning calorimetry (DSC) was performed with a computer-controlled Phoenix DSC 204 F1 thermal analyzer (Netzsch, Selb, D) with argon as protecting gas. The samples were placed in aluminum pans which were cold-sealed. Experimental data are displayed in such a way that exothermic peaks occur at negative heat flow and endothermic peaks at positive heat flow. The given temperatures correspond to the onset of the respective thermal process.

Polarizing Optical Microscopy: Optical analyses were made by heated-stage polarized optical microscopy (POM) with an Axio Imager A1 microscope (Carl Zeiss MicroImaging GmbH, Göttingen, D) equipped with a hot stage, THMS600 (Linkam Scientific Instruments Ltd, Surrey, UK), and temperature controller Linkam TMS 94 (Linkam Scientific Instruments Ltd, Surrey, UK). The images were recorded as movies with a digital camera after initial heating during the cooling stage.

Crystal Structure Analysis: A few crystals of **2c** were selected at about 0 °C under a perfluorinated polyether (viscosity 1600 cSt, ABCR GmbH, Karlsruhe, D) with the help of an optical microscope. The best specimen was chosen and adhered to a glass capillary with the help of the oil and a complete intensity data set was collected with the aid of a Bruker Smart 1000 single-crystal X-ray diffractometer (Bruker, Karlsruhe, D) with graphite monochromated Mo-K_α radiation (λ = 0.71073 Å) at –60 °C. Data reduction was carried out with the program package SAINT,[30] and a numerical absorption correction was performed with the program SADABS.[31] Crystal structure solution by direct methods with SIR92[32] yielded the heavy atom positions. Subsequent difference Fourier analyses and least-squares refinement with SHELXL-97[33] allowed for the location of the remaining atom positions. In the final step of the crystal structure, refinement hydrogen atoms of idealized –CH_2 and –CH_3 groups were added and treated with the riding atom mode; their isotropic displacement factor was chosen as 1.2 times the preceding carbon atom. For further information see the Supporting Information. CCDC-682994 contains the supplementary crystallographic data for **1c**. These data can be obtained free of charge from The Cambridge Crystallographic Data Centre via www.ccdc.cam.ac.uk/data_request/cif. For drawings of the crystal structure the program Diamond was used.[34]

Supporting Information (see footnote on the first page of this article): Information on the crystal structure solution and refinement of $[C_{12}mim]_3[TbBr_6] \cdot 2CH_3CN$, additional graphical representation of vibrational spectra, and data regarding the thermal behavior of all compounds.

Acknowledgments

This work was supported by the Deutsche Forschungsgemeinschaft (DFG) in the priority program SPP 1191 "Ionic Liquids". A. G. and A.-V. M. thank the Fonds der Chemischen Industrie for a Doktoranden- and a Dozentenstipendium, respectively. Dr. Klaus Merz is acknowledged for X-ray data collection.

[1] P. Wasserscheid, T. Welton, (Eds.) *Ionic Liquids in Synthesis*, Wiley-VCH, Weinheim, 2nd ed., **2008**.
[2] N. V. Plechkova, K. R. Seddon, *Chem. Soc. Rev.* **2008**, *37*, 123.
[3] X. Wang, F. W. Heinemann, M. Yang, B. Melcher, M. Fekete, A.-V. Mudring, P. Wasserscheid, K. Meyer, *Chem. Commun.* **2009**, 7405.
[4] C. M. Gordon, J. D. Holbrey, A. R. Kennedy, K. R. Seddon, *J. Mater. Chem.* **1998**, *8*, 2627.
[5] a) J. D. Holbrey, K. R. Seddon, *J. Chem. Soc., Dalton Trans.* **1999**, 2133; b) A. E. Bradley, C. Hardacre, J. D. Holbrey, S. Johnston, S. E. J. McMath, M. Nieuwenhuyzen, *Chem. Mater.* **2002**, *14*, 629; c) J. De Roche, C. M. Gordon, C. T. Imrie, M. D. Ingram, A. R. Kennedy, F. L. Celso, A. Triolo, *Chem. Mater.* **2003**, *15*, 3089; d) D. M. Fox, W. H. Awad, J. W. Gilman, P. H. Maupin, H. C. De Long, P. C. Trulove, *Green Chem.* **2003**, *5*, 724; e) K.-M. Lee, Y.-T. Lee, I. J. B. Lin, *J. Mater. Chem.* **2003**, *13*, 1079; f) A. Downard, M. J. Earle, C. Hardacre, S. E. J. McMath, M. Nieuwenhuyzen, S. J. Teat, *Chem. Mater.* **2004**, *16*, 43; g) J. Dupont, P. A. Z. Suarez, *Phys. Chem. Chem. Phys.* **2006**, *8*, 2441; h) K. Goossens, P. Nockemann, K. Driesen, B. Goderis, C. Görller-Walrand, K. Van Hecke, L. Van Meervelt,

 © 2011 Wiley-VCH Verlag GmbH & Co. KGaA, Weinheim

E. Pouzet, K. Binnemans, T. Cardinaels, *Chem. Mater.* **2008**, *20*, 157.

[6] a) K. Goossens, K. Lava, P. Nockemann, K. Van Hecke, L. Van Meervelt, P. Pattison, K. Binnemans, Th. Cardinaels, *Langmuir* **2009**, *25*, 5881; b) A. Getsis, A.-V. Mudring, *Z. Anorg. Allg. Chem.* **2009**, *635*, 2214.

[7] a) J. L. Serrano (Ed.), *Metallomesogens, Synthesis Properties and Applications*, Wiley-VCH, Weinheim, **1996**; b) F. Neve, *Adv. Mater.* **1996**, *8*, 277; c) B. Donnio, D. W. Bruce, "Metallomesogens" in *Liquid Crystals II* (Ed.: D. M. P. Mingos), Springer, Berlin, **1999**, p. 193; d) R. Giménez, D. P. Lydon, J. L. Serrano, *Curr. Opin. Solid State Mater. Sci.* **2002**, *6*, 527; e) I. J. B. Lin, C. S. Vasam, *J. Organomet. Chem.* **2005**, *690*, 3498.

[8] a) P. Espinet, M. A. Esteruelas, L. A. Oro, J. L. Serrano, E. Sola, *Coord. Chem. Rev.* **1992**, *117*, 215; b) F. Neve, *Adv. Mater.* **1996**, *8*, 277; c) P. J. Alonso, *Metallomesogens* **1996**, 387; d) P. J. Alonso, *Metallomesogens* **1996**, 349; e) N. Hoshino, *Coord. Chem. Rev.* **1998**, *174*, 77; f) I. J. B. Lin, C. S. Vasam, *J. Organomet. Chem.* **2005**, *690*, 3498.

[9] a) K. Binnemans, C. Görller-Walrand, *Chem. Rev.* **2002**, *102*, 2303; b) C. Piguet, J. C. G. Bünzli, B. Donnio, D. Guillon, *Chem. Commun.* **2006**, 3755; c) E. Terazzi, S. Suarez, S. Torelli, H. Nozary, D. Imbert, O. Mamula, J.-P. Rivera, E. Guillet, J. M. Bénech, G. Bernardinelli, R. Scopelliti, B. Donnio, D. Guillon, J.-C. G. Bünzli, C. Piguet, *Adv. Funct. Mater.* **2006**, *16*, 157.

[10] A.-V. Mudring, S. Tang, *Eur. J. Inorg. Chem.* **2010**, *18*, 2569.

[11] M. Grell, D. C. Bradley, *Adv. Mater.* **1999**, *11*, 895; M. O′Neill, S. M. Kelley, *Adv. Mater.* **2003**, *15*, 1135.

[12] a) L. N. Puntus, K. J. Schenk, J. C. G. Bünzli, *Eur. J. Inorg. Chem.* **2005**, *23*, 4739; b) J. Kocher, F. Gumy, A.-S. Chauvin, J. C. G. Bünzli, *J. Mater. Chem.* **2007**, *17*, 654; c) A. Getsis, A.-V. Mudring, *Z. Anorg. Allg. Chem.* **2010**, *636*, 1726.

[13] a) Y. G. Galyametdinov, W. Haase, B. Goderis, D. Moors, K. Driesen, R. Van Deun, K. Binnemans, *J. Phys. Chem. B* **2007**, *111*, 13881; b) Y. G. Galyametdinov, A. A. Knyazev, V. I. Dzhabarov, T. Cardinaels, K. Driesen, C. Görller-Walrand, K. Binnemans, *Adv. Mater.* **2008**, *20*, 252.

[14] a) Y. Galyametdinov, M. A. Athanassopoulou, K. Griesar, O. Kharitonova, E. A. Soto Busmante, L. Tinchurina, I. Ovchinnikov, I. W. Haase, *Chem. Mater.* **1996**, *8*, 922; b) Y. Galyametdinov, G. Ivanova, I. Ovchinnikov, A. Prosvirin, D. Guillon, B. Heinrich, D. A. Dunmur, D. W. Bruce, *Liq. Cryst.* **1996**, *20*, 831; c) K. Binnemans, Y. G. Galyametdinov, R. Van Deun, D. W. Bruce, S. R. Collinson, A. P. Polishchuk, I. Bikchantaev, W. Haase, A. V. Prosvirin, L. Tinchurina, I. Litvinov, A. Gubajdullin, A. Rakhmatullin, K. Uytterhoeven, L. Van Meervelt, *J. Am. Chem. Soc.* **2000**, *122*, 4335; d) V. S. Mironov, Y. G. Galyametdinov, A. Ceulemans, K. Binnemans, *J. Chem. Phys.* **2000**, *113*, 10293; e) Y. G. Galyametdinov, W. Haase, L. Malykhina, A. Prosvirin, I. Bikchantaev, A. Rakhmatullin, K. Binnemans, *Chem. Eur. J.* **2001**, *7*, 99; f) K. Binnemans, L. Malykhina, V. S. Mironov, W. Haase, K. Driesen, R. Van Deun, L. Fluyt, C. Görller-Walrand, Y. G. Galyametdinov, *ChemPhysChem* **2001**, *2*, 680.

[15] A. Getsis, B. Balke, C. Felser, A.-V. Mudring, *Cryst. Growth Des.* **2009**, *9*, 4429.

[16] A. Bohnsack, G. Meyer, *Z. Kristallogr. New Cryst. Structures* **1997**, 212, 2.

[17] a) A. Babai, A.-V. Mudring, *Acta Crystallogr., Sect. E* **2005**, *61*, o2913; b) A. Babai, A.-V. Mudring, *Chem. Mater.* **2005**, *17*, 6230; c) A. Babai, A.-V. Mudring, *Inorg. Chem.* **2006**, *45*, 3249; d) A. Babai, A.-V. Mudring, *Dalton Trans.* **2006**, 1828; e) A. Babai, A.-V. Mudring, *J. Alloys Compd.* **2006**, *418*, 122; f) A. Babai, A.-V. Mudring, *Z. Anorg. Allg. Chem.* **2006**, *632*, 1956; g) A. Babai, A.-V. Mudring, *Inorg. Chem.* **2006**, *45*, 4874.

[18] J. De Roche, C. M. Gordon, C. T. Imrie, M. D. Ingram, A. R. Kennedy, F. Lo Celso, A. Triolo, *Chem. Mater.* **2003**, *15*, 3089.

[19] T. Steiner, *Acta Crystallogr., Sect. B* **1998**, *54*, 456.

[20] a) A. Getsis, A.-V. Mudring, *Acta Crystallogr., Sect. E.* **2005**, *61*, o2945; b) A. Getsis, A.-V. Mudring, *Cryst. Res. Technol.* **2008**, *43*, 2214.

[21] W. Kiefer, "Raman-Spektroskopie" in *Spektroskopie amorpher und kristalliner Festkörper* (Eds.: D. Haarer, H. W. Spiess), Steinkoppf-Verlag, Darmstadt, **1995**.

[22] K. Binnemans, *Chem. Rev.* **2005**, *105*, 4148.

[23] W. Dobbs, L. Douce, L. Allouche, A. Louati, F. Malbosc, R. Welter, *New J. Chem.* **2006**, *30*, 528.

[24] A. Kanazawa, T. Ikeda, *Chem. Mater.* **2000**, *12*, 3776.

[25] B. Henderson, G. F. Imbusch, *Optical Spectroscopy of Inorganic Solids*, Clarendon Press, Oxford, **1989**.

[26] L. J. Nugent, R. D. Baybarz, J. L. Burnett, *J. Phys. Chem.* **1973**, *77*, 1528.

[27] G. H. Dieke, *Spectra and Energy Levels of Rare Earth Ions in Crystals*, Interscience Publishers, New York, **1968**; W. T. Carnall, H. M. Crosswhite, H. Crosswhite, *Energy Level Structure and Transition Probabilities in the Spectra of Trivalent Lanthanides in LaF_3*, Special Report **1977** (Argonne, IL: Chemistry Division, Argonne National Laboratory).

[28] E. Guillet, D. Imbert, R. Scopelliti, J. C. G. Bünzli, *Chem. Mater.* **2004**, *16*, 4063.

[29] G. Meyer, S. Dötsch, Th. Staffel, *J. Less – Common Met.* **1987**, *127*, 155.

[30] *Software Package SMART and SAINT*, Siemens Analytical X-ray Instruments Inc., Madison, WI, **1996**.

[31] G. M. Sheldrick, *SADABS*, University of Göttingen, Göttingen, Germany, **1995**.

[32] *SIR92 – A Program for Crystal Structure Solution*, A. Altomare, G. Cascarano, C. Giacovazzo, A. Guagliardi, *J. Appl. Crystallogr.* **1993**, *26*, 343.

[33] *SHELXL-97*, W. S. Sheldrick, University of Göttingen, Göttingen, Germany, **1997**.

[34] *DIAMOND*, Crystal Impact, Bonn, **1995**.

Received: February 20, 2011
Published Online: June 17, 2011

 © 2011 Wiley-VCH Verlag GmbH & Co. KGaA, Weinheim